# A Liquid Piston Stirling Engine with Float-Type Linear Alternator for Electricity Generation: An Effect of Coil Geometry

Eko Yuwono Putro[1], Prastowo Murti[1,*], Adhika Widyaparaga[1] and I Made Miasa[1]

[1] Department of Mechanical and Industrial Engineering, Universitas Gadjah Mada, Jl. Grafika No. 2, Yogyakarta 55281, Indonesia
* prastowomurti@ugm.ac.id

**Abstract.** Liquid Piston Stirling Engine (LPSE), also known as the Fluidyne engine, is a simple external combustion engine that converts low-temperature thermal energy into mechanical oscillations using air and water as working fluids. While previous applications of LPSE have primarily focused on water pumping in remote areas, its potential for electricity generation remains largely unexplored. This study experimentally demonstrates the feasibility of generating electricity using an LPSE equipped with a float-type linear alternator. The experimental setup consists of an LPSE and a simple linear alternator using a floating permanent magnet. Various coil configurations were tested to optimize the induced voltage output. Results show that the integration of the linear alternator has minimal impact on the LPSE's performance, with onset temperature increasing by only 10 K. The highest induced voltage was achieved with a coil using 0.15 mm wire diameter and 25 mm length, generating a maximum power output of 2.27 mW at an optimal load resistance of 450 Ω. These findings validate the LPSE's potential as a simple solution for electricity generation in remote and off-grid areas.

**Keywords:** Liquid Piston, Linear Alternator, Electric Generator.

## 1 Introduction

Access to reliable electricity remains a critical challenge in many remote and off-grid areas due to limited infrastructure and high costs associated with conventional power generation methods [1,2]. Low-grade thermal energy sources such as biomass combustion or solar heat are abundant but often underutilized for sustainable energy production. One of the solutions is utilizing an external combustion engine called liquid piston Stirling engine (LPSE), also known as the Fluidyne engine. It offers a simple and cost-effective means of converting low-temperature thermal energy into acoustic energy, using air and water as the working fluids [3]. Several studies have shown that this engine requires a temperature difference of less than 100 K to initiate spontaneous oscillations of the gas and liquid columns (onset temperature) [4–6]. This engine consists of a looped column and tuning columns. Half of the looped column is filled


M. Rafieiy et al. (eds.), *Proceedings of the 8th Mechanical and Industrial Engineering Symposium (MIE 2025)*, Atlantis Highlights in Engineering 42,
https://doi.org/10.2991/978-94-6239-687-6_4

with liquid, while the remaining portion contains air at atmospheric pressure and temperature. One end of each tuning column is open to the environment.

The application of the LPSE was first demonstrated by C. West, who used it as a water pump [7]. A laboratory prototype of the LPSE achieved a pumping head of 3.05 meters and a flow rate of 1.7 $m^3 \cdot h^{-1}$ with an input heating power of 297 W. Further research and development may enable the use of Fluidyne water pumps in remote, off-grid areas due to their extremely simple design that eliminates the need for solid pistons [8,9]. In addition to water pumping, the oscillations of the liquid column can also be utilized to generate electricity by incorporating a simple linear alternator. In a previous study, our group numerically demonstrated that electricity can be generated by placing a floating magnet inside the liquid column and winding a coil on the outside of the tube called float-type linear alternator [10]. However, this concept has not yet been realized experimentally.

Therefore, this study aims to experimentally demonstrate a liquid piston Stirling engine equipped with a float-type linear alternator for electricity generation. The influence of installing the float-type linear alternator on the minimum temperature difference required to induce spontaneous oscillations (onset temperature) is analyzed. Additionally, the coil configuration is examined to determine the optimum induced voltage.

## 2 Experimental Method

### 2.1 System Design

Fig. 1 shows the experimental apparatus, which consists of a LPSE) and a simple linear alternator. The LPSE has a looped column with a total length of 2660 mm and a diameter of 36 mm. The tuning column has a length of 2000 mm and a diameter of 11.8 mm. The regenerator is composed of a series of stainless-steel wire mesh screens with a mesh number of 30, cut into circular shapes with a diameter of 36 mm and assembled to a total length of 70 mm. The hot and ambient heat exchangers are made of brass cylindrical blocks with axial holes 3.5 mm in diameter. The hot heat exchanger is 85 mm long, while the ambient heat exchanger is 100 mm long. The hot heat exchanger is heated by an electric heater with a maximum power of 400 W, while the ambient heat exchanger is cooled by circulating water maintained at a temperature of 293 K. The working fluids consisted of 1.5 liters of distilled water and air at ambient temperature and atmospheric pressure.

As illustrated in Fig. 1, the linear alternator consisted of a permanent magnet placed inside a liquid column and a surrounding solenoid coil. In this setup, the alternator was mounted on one end of a column. The permanent magnet used was a cylindrical Neodymium Magnet (NdFeB) N52 with a diameter of 29 mm and height of 25 mm, a magnetic flux density of 0.5086 mT, and axial magnetization. A Styrofoam cylinder, 30 mm in diameter and 180 mm in height, was attached to the magnet to act as a float. This combination resulted in an overall density of 970 $kg \cdot m^{-3}$, matching that of water, which allowed the magnet to float and move with the oscillations of the liquid column. The shape of the coil in an alternator significantly impacts its performance, primarily by influencing the generated voltage. A well-designed coil—with a specific shape and

number of turns—maximizes the effectiveness of the electromagnetic induction process, leading to stable and efficient power output. In this study, we used several types of 1000 turns coils with different wire diameters ($d$) and coil lengths ($L_C$), as summarized in Table 1.

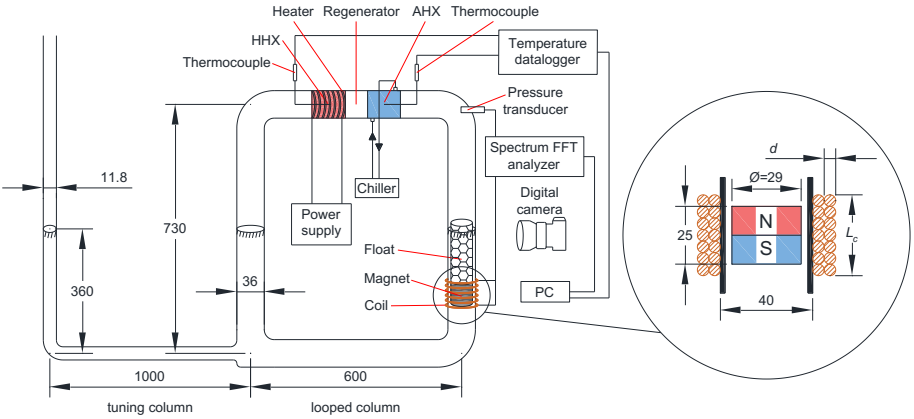


**Fig. 1.** Schematic diagram of liquid piston Stirling engine with float-type linear alternator.

**Table 1.** Coil Geometries.

| Coil | Wire diameter in mm ($d$) | Coil height in mm ($L_C$) |
|---|---|---|
| 1 | 0.15 | 25 |
| 2 | 0.30 | 25 |
| 3 | 0.45 | 25 |
| 4 | 0.60 | 25 |
| 5 | 0.15 | 50 |
| 6 | 0.15 | 75 |
| 7 | 0.15 | 100 |

## 2.2 Measurement method

Temperature measurements at both ends of the regenerator were obtained using two type-K thermocouples. These were connected to a high-precision USB data acquisition device (Digilent MCC USB-2408-2AO) and continuously monitored through a PC. Pressure oscillations within the gas column were detected by a pressure transducer (102A05, PCB Piezotronics) positioned at the 90° elbow and linked to an FFT analyzer (Onosokki DS-3000). The displacement of the liquid column was recorded with a digital camera and analyzed using video analysis software (Tracker) [11]. The induced voltage was measured using probes clamped directly to the coil leads, with the signals sent to the same FFT analyzer and streamed to a PC for data acquisition. A potentiometer used as the electrical load, allowing for the measurement of the generated electrical power.

To assess the impact of installing a float-type linear alternator on the onset temperature of the LPSE, we measured the system's quality factor ($Q$). A short pulse was applied to the LPSE via the tuning column to generate a pressure waveform at a given temperature ratio ($T_H/T_A$). The ambient side of the regenerator $T_A$ was maintained at 293 K, while the hot side $T_H$ was gradually increased in 30 K increments starting from ambient temperature. The pressure waveform was transformed to the amplitude spectrum via a fast Fourier transform algorithm. From these curves, the quality factor was determined by $Q = f_0/\Delta f$, where $f_0$ is the peak frequency and $\Delta f$ is the full width at half maximum (FWHM) of the spectrum [12].

## 3 Results and Discussion

### 3.1 The Effect of Installation of Float-Type Linear Alternator on LPSE Performance

Fig. 2 presents the inverse quality factor ($1/Q$) as a function of the temperature ratio ($T_H/T_A$) for the LPSE system, both with and without the float-type linear alternator. These measurements were taken under open-circuit conditions for the solenoid coil. The results show that $1/Q$ decreases with increasing $T_H/T_A$ in both configurations. The LPSE equipped with the linear alternator reaches $1/Q = 0$ at a temperature ratio of approximately 1.40, while the LPSE without the alternator reaches this point at around 1.38. A value of $1/Q = 0$ indicates the temperature ratio at which the acoustic power generated in the regenerator becomes sufficient to offset the total energy dissipation in the system, leading to self-sustained oscillations. The observed difference in onset temperature ratios between the two cases is about 0.02, corresponding to roughly 10 K, which is relatively small difference compare to other thermoacoustic engine[13].

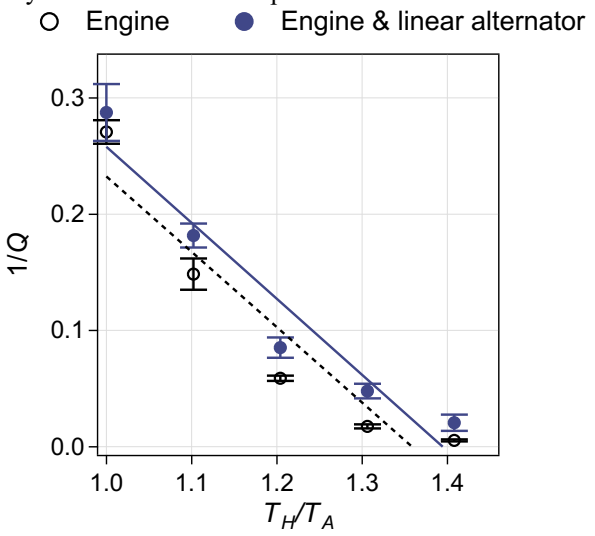


**Fig. 2.** $1/Q$ as a function of temperature ratio ($T_H/T_A$). The line and dash-line are the fitting data points.

Once self-sustained oscillation begins, the pressure amplitude, liquid column displacement, and oscillation frequency of the LPSE—with and without the linear alternator—were measured as the temperature ratio increased, as shown in Fig. 3 (a)-(c). As seen in Fig. 3 (a), the pressure amplitude for both configurations increases similarly with rising $T_H/T_A$, reaching a maximum of approximately 2.4 kPa at a temperature ratio of 1.95. A similar trend is observed for the liquid column displacement and oscillation frequency in Fig. 3 (b) and (c), respectively, where both values increase with $T_H/T_A$. At $T_H/T_A$= 1.95, the maximum displacement was 73 mm, and the oscillation frequency was 0.62 Hz. Based on the results for onset temperature, pressure amplitude, liquid piston displacement, and oscillation frequency, we conclude that the installation of the float-type linear alternator does not impose a significant load on the LPSE system.

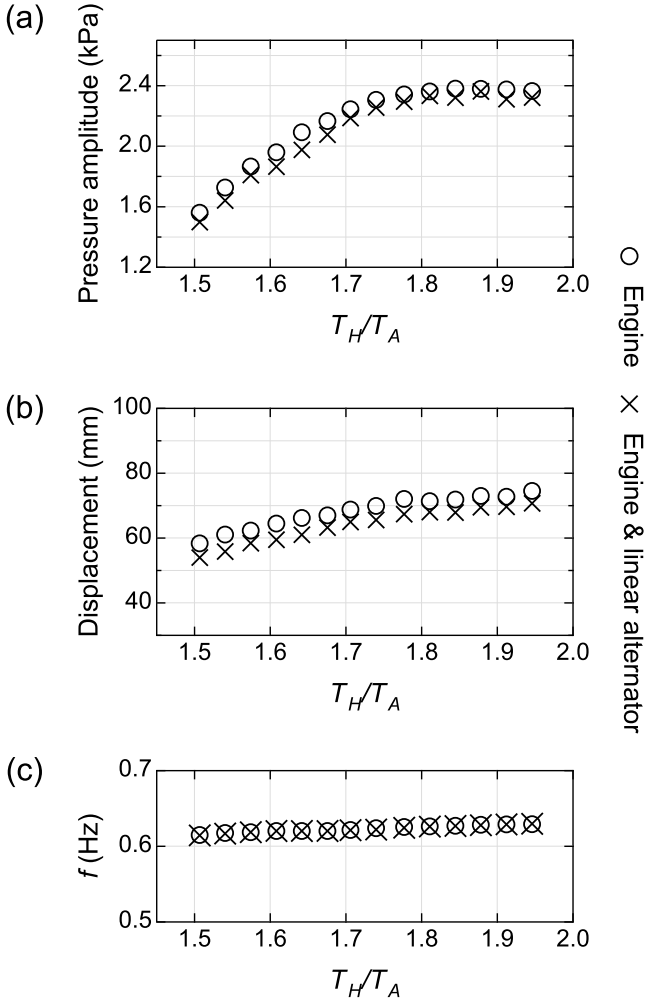


**Fig. 3.** a) Pressure amplitude, (b) liquid column displacement, and (c) oscillation frequency as a function of temperature ratio ($T_H/T_A$).

### 3.2 Induced Voltage on Open Circuit Condition on Different Coil Wire Diameter

The induced voltage was measured while varying the coil wire diameter from 0.15 mm to 0.6 mm, corresponding to coils 1, 2, 3, and 4, respectively, as detailed in Table 1. The coil length was kept constant at 25 mm throughout the experiment, which was conducted under open-circuit conditions. Fig. 4 (a) presents the induced voltage waveforms at a temperature ratio of $T_H/T_A$= 1.94 for each coil. The highest peak voltage, approximately 3.3 V, was observed for the coil with a 0.15 mm wire diameter, while coils with larger wire diameters produced progressively lower voltage amplitudes. This reduction is due to the increase in the radius of each coil turn, which will decrease the rate of change of magnetic flux for each turn, thereby decreasing the induced voltage. Fig. 4 (b) shows the peak voltage as a function of temperature ratio across these coil types. For all diameters, voltage increases nearly linearly with temperature ratio, but the 0.15 mm coil consistently outperforms others. These results confirm that thinner coil wire with more compact turns enhances electromagnetic coupling, yielding greater voltage output under identical thermal conditions.

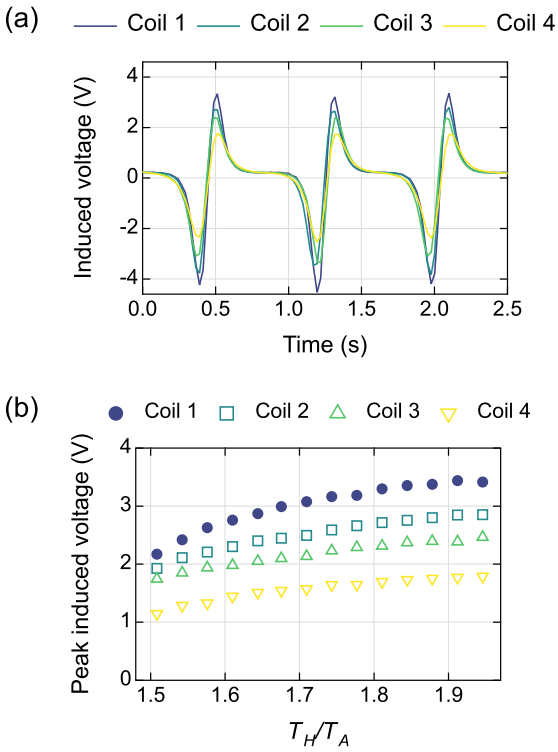


**Fig. 4.** Induced voltage under open-circuit condition for various coil wire diameters: (a) Time-domain waveform at maximum temperature ratio ($T_H/T_A$ = 1.95), (b) Peak induced voltage as a function of temperature ratio ($T_H/T_A$).

### 3.3 Induced Voltage on Open Circuit Condition on Different Coil Length

As the permanent magnet oscillates axially relative to the solenoid coil, we conducted experiments using coils of different lengths, represented by coils 1, 5, 6, and 7, respectively. Fig. 5 (a) shows the no-load voltage waveforms at a temperature ratio of $T_H/T_A$= 1.95 for each coil. Coil 1 produced the highest voltage peak, while the longest coil (coil 7) exhibited the lowest amplitude. This behavior can be attributed to the fact that only a limited section of the coil is effectively positioned to experience the varying magnetic field during oscillation. In longer coils, many turns fall outside the effective stroke range of the moving magnet and contribute minimally to the total induced voltage. Fig. 5 (b) presents the peak voltage as a function of temperature ratio for all coil lengths. Coil 1 consistently delivers the highest voltage across the tested range. While all configurations show a linear increase in voltage with rising temperature ratio, the reduced performance of longer coils highlights the importance of aligning coil geometry with the magnet's displacement range.

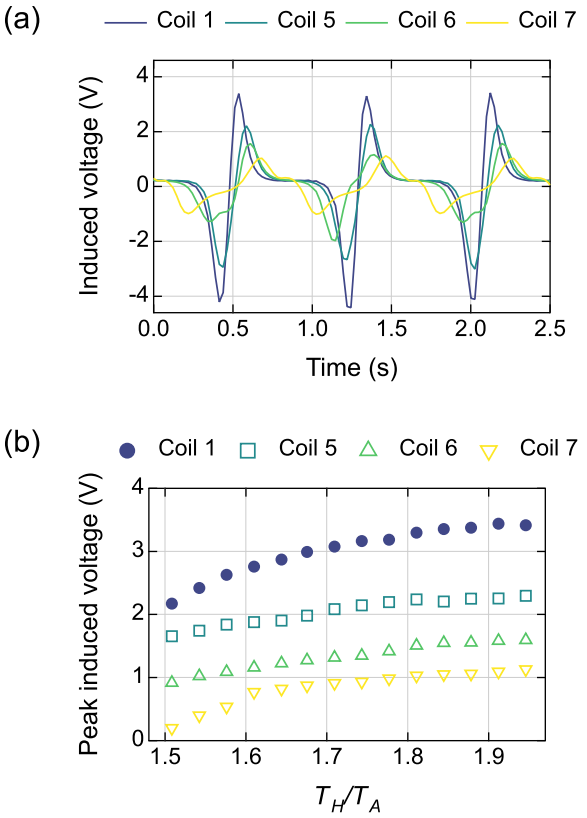


**Fig. 5.** Induced voltage under open-circuit condition for various coil length: (a) Time-domain waveform at maximum temperature ratio ($T_H/T_A$ = 1.95), (b) Peak induced voltage as a function of temperature ratio ($T_H/T_A$).

### 3.4 Output Electricity with Different Load Resistance

To measure the electrical energy generated by the linear alternator, a potentiometer was connected across both ends of the coil wire, using coil 1 at a temperature ratio of $T_H/T_A$ = 1.95, as it produced the highest induced voltage. The load resistance was varied from 50 Ω to 1000 Ω to identify the value that best matched the coil's impedance, thereby maximizing power output. Assuming a purely resistive circuit with negligible reactance and inductance, the electrical power output was calculated using the following formula (1). Where $T$ is the period of induced voltage, $N_T$ is the number of sampling points in one period, $V(t)$ is amplitude of the induced voltage, $\Delta t$ is the sampling interval, and $R$ is the value of the external load resistance.

$$W = \frac{1}{T}\sum_{n=0}^{N_T}\frac{|V(t)|^2}{R}\Delta t \tag{1}$$

As shown in Fig. 6, the output power increased with load resistance, peaking at 2.27 mW at 450 Ω, before decreasing at higher resistance values. At low resistance, higher current flow generates a stronger opposing magnetic field as described by Lenz's Law. Resulting in a larger Lorentz force that resists the magnet's motion. This increased electromagnetic damping slows down oscillation and shortens the stroke length, reducing the rate of magnetic flux change through the coil. As a result, the induced voltage drops, limiting power output despite the high current. At high resistance, the lower current reduces damping, but the limited current flow also restricts power. Therefore, maximum power occurs at an intermediate resistance where voltage and current are optimally balanced.

Based on the observed symmetry of the oscillatory motion, it is hypothesized that installing linear alternators on both vertical column of the LPSE could potentially double the electrical output, yielding an estimated power of approximately 4.54 mW. Additionally, improvements in magnetic coupling such as the application of Halbach array magnet configurations may further enhance the induced voltage. These considerations present promising directions for future design optimization but remain to be verified through experimentation.

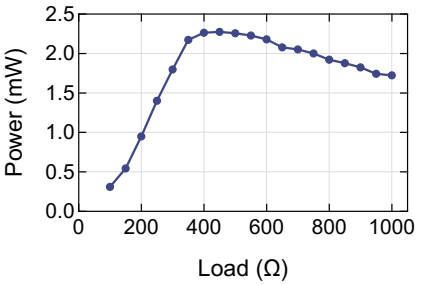


**Fig. 6.** Electrical power output as a function of electrical load for coil No. 1 with 0.15 mm wire diameter and 25 mm length at maximum temperature ratio ($T_H/T_A$=1.95).

## 4 Conclusion

This study experimentally investigates the feasibility of generating electricity using a liquid piston Stirling engine (LPSE) coupled with a linear generator. The findings demonstrate that the LPSE maintains stable oscillations when integrated with the linear alternator, with increased temperature ratios enhancing pressure amplitude and liquid-column displacement. Additionally, coil design parameters significantly influence induced voltage output, where thinner wire diameters and shorter coil lengths improve peak induced voltage. Load testing identified an optimal external resistance of 450 Ω, yielding maximum power output of 2.27 mW. These results provide valuable insights for optimizing LPSE-based energy conversion systems.

## Acknowledgement

This study was supported by the Fundamental Research Scheme of the Directorate General of Higher Education, Research and Technology, Ministry of Education, Culture, Research and Technology, the Republic of Indonesia number 2416/UN1/DITLIT/Dit-Lit/PT.01.03/2025.

## References

1. Rachmawan. Budiarto, D. Sulistyo. Widhyarto, and Muhammad. Sulaiman, Transisi Energi Berbasis Komunitas Di Kepulauan Dan Wilayah Terpencil = Community-Based Energy Transition in Islands and Remote Areas (Universitas Gadjah Mada, 2019)
2. N. Gothwal, T. Manglani, and D. K. Doda, Importance of Off-Grid Power Generation Using Renewable Energy Resources-A Review (2018)
3. Colin D. West, Liquid Piston Stirling Engines, illustrated (Van Nostrand Reinhold, 1983)
4. S. Tamura, H. Hyodo, and T. Biwa, Jpn J Appl Phys 58, (2019)
5. H. Hyodo, S. Tamura, and T. Biwa, J Appl Phys 122, (2017)
6. M. Ito, P. Murti, S. Tsuboi, E. Shoji, and T. Biwa, J Acoust Soc Am 151, (2022)

7. C. D. West and R. B. Pandey, in Proceedings of the Intersociety Energy Conversion Engineering Conference (1981)
8. E. Orda and K. Mahkamov, J Sol Energy Eng 126, 768 (2004)
9. M. Aliyu, G. Hassan, S. A. Said, M. U. Siddiqui, A. T. Alawami, and I. M. Elamin, Renewable and Sustainable Energy Reviews 87, 61 (2018)
10. W. D. Astuti and P. Murti, Journal of the Brazilian Society of Mechanical Sciences and Engineering 46, 579 (2024)
11. D. Brown and A. J. Cox, Phys Teach 47, 145 (2009)
12. T. Biwa, Introduction to Thermoacoustics Devices (World Scientific Publishing Co. Inc., 2021)
13. P. Murti, I. Setiawan, J. Z. Rosafira, A. Widyaparaga, W. D. Astuti, and T. Biwa, International Journal of Renewable Energy Development 13, 708 (2024)